HL-LHC MAGNETS FIELD QUALITY: CURRENT SITUATION, STRATEGIES AND MITIGATION MEASURES*

A. Fornara†, R. De Maria, L. Fiscarelli, G. Iadarola, M. Giovannozzi, S. Izquierdo Bermudez, E. H. Maclean, K. Skoufaris, G. Sterbini, R. Tomás García, CERN, Meyrin, Switzerland

Abstract

The production of the new superconducting magnets for the luminosity upgrade of the LHC is in full swing. The performance of the magnets is probed by means of detailed magnetic measurements of the transfer function and field quality of the various families of magnets, i.e. triplet quadrupoles and separation and recombination dipoles. In this paper, the current situation in terms of magnetic properties is presented and reviewed in detail. Furthermore, dedicated beam dynamics simulations to address the possible issues for the various families of magnets are presented.

INTRODUCTION

The luminosity upgrade of the CERN Large Hadron Collider (HL-LHC) [1, 2] involves, among other changes, a complete revision of the layout of the interaction regions (IR) for the ATLAS and CMS experiments. The inner triplet quadrupoles, separation, and recombination dipoles will be replaced by new hardware, and crab cavities (CC) will be added. A construction programme, shared among the collaborating institutes, is in full swing, and the production of the new devices is progressing well. An ambitious programme of magnetic measurements is also underway with the goal of providing detailed information about the performance of the magnets and their field quality (FQ). The large volume of data obtained from the magnetic measurements is impressive and, beyond offering an early indication of magnet performance, it can also be used to optimise the installation sequence by enabling the sorting of the magnets. This approach has been explored in the design phase of various modern accelerators (see, e.g. Refs. [3–13]) and has been implemented with success in the CERN LHC [14–16].

Similarly to LHC, sorting is foreseen for the new insertion magnets of HL-LHC and preliminary studies were carried out considering the many possible permutations of triplet quadrupoles [17]. Ideally, a sorting scheme relies on a large pool of magnets, from which subsets are selected and optimally assigned to the most suitable positions in the ring. Unlike LHC, the magnet families for HL-LHC comprise a small number of magnets, which is certainly suboptimal for any sorting approach. Furthermore, severe hardware and scheduling constraints need to be taken into account. The most recent results for the sorting options for the Q2 triplet quadrupole, including currently known constraints, can be found in Ref. [18]. Here, we focus on the current status of magnetic measurements for the Q1/Q3 triplet quadrupoles and the D2 recombination dipoles. These data were then used to devise the optimal allocation of the currently available magnets, and the recommended positions are presented and discussed in detail in this paper.

As a last point, we recall that a sorting algorithm relies on a physical observable that is used as a figure of merit of a given sequence of magnets with a certain FQ. For the case of the Q2, which are split into two cryo-assembly (CA) powered in series, the criterion has been to pair CAs for similar transfer functions to minimise beta-beating. As an additional observable, the amplitude detuning has been considered and minimised, in view of easing the initial beam commissioning. Each Q1 or Q3 CA is made of two magnets, but each CA is independently powered. Hence, beta-beating is not an issue, and the amplitude detuning has been the physical observable to guide the sorting strategy. As far as the D2 dipoles are concerned, the skew-quadrupole component turned out to be the property to be controlled and the observables related with linear coupling have been used for assessing the best slot for the D2s. It is worth noting that the case of the D1 separation dipoles will be considered next, but the presence of a corrector package, housing several linear and non-linear corrector magnets, installed next to the D1 provides an effective means to control the FQ of the D1s. Hence, sorting might be of limited use in that case.

MAGNETIC MEASUREMENTS FOR HL-LHC MAGNETS

The magnetic characterisation of the HL-LHC IR magnets (see Fig. 2 of Chapter 5 in Ref. [2]) is performed during and after production and assembly, at ambient temperature (warm) and at 1.9 K (cold). The results of cold measurements are from the magnet in the vertical test stand or, when available, on the final CA in horizontal configuration, and the latter is taken as the reference whenever it exists. In the absence of cold measurements, the field quality is extrapolated from warm measurements. The measured field harmonics are used as input for beam simulations and form the basis of the sorting strategies discussed in the following sections (see also Ref. [18]). Multipoles are expressed in the magnet reference frame (looking at the magnet from the connection side) and are quoted in units, where one unit is 10^{-4} of the main field at the reference radius R_{ref}, which is taken as $1/3$ of the cold-bore aperture. The status of the measurement campaign for each family is summarised in Table 1 and the FQ plots referenced in the table show the integral harmonics at nominal current.

The Q1 and Q3 quadrupoles CA [19, 20] are made of two MQXFA magnets each, first tested individually in the vertical stand and then re-tested once integrated (see

* Work supported by the HL-LHC project
† andrea.fornara@cern.ch

Table 1: Status of the magnetic measurements of the HL-LHC IR magnet families.

Family	I_{nom} [kA]	R_{ref} [mm]	Units	Measurement status	FQ Fig.
MQXFA	16.23	50	16	16 vertical-cold, 6 in final CA	1a
MQXFB	16.23	50	10	9 warm, 7 cold in final CA; 2 extrapolated	1b
MBRD	12.33	35	6	5 warm, 2 cold in final CA; 3 extrapolated	1c

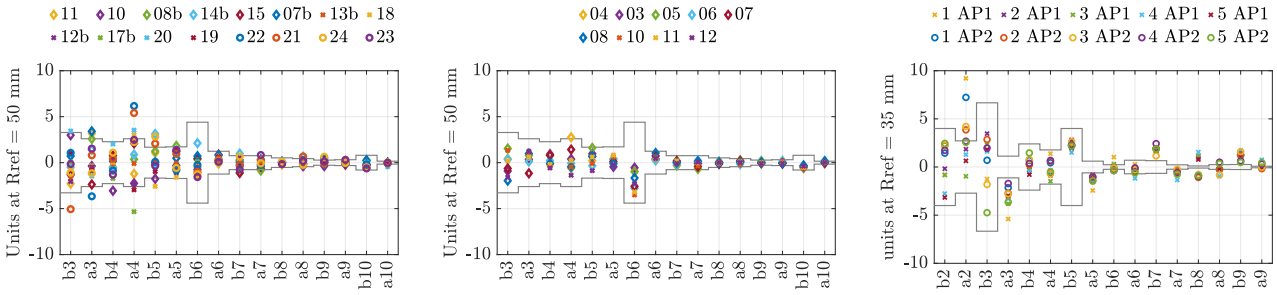

(a) MQXFA (Q1/Q3) (b) MQXFB (Q2) (c) MBRD (D2 main)

Figure 1: Integral field harmonics at I_{nom} for the magnet families relevant to this study: (a) MQXFA [19], (b) MQXFB, (c) MBRD. The gray lines indicate the FQ values of the acceptance criteria.

Fig. 1a). The Q2 quadrupoles are made by a single MQXFB quadrupole [21] (see Fig. 1b), each housed in a CA together with nested MCBXFB orbit correctors to provide control of the horizontal and vertical beam orbits. The D2 CA comprises an MBRD recombination dipole (see Fig. 1c) and two MCBRD orbit correctors. The orbit correctors (MCBXFB and MCBRD) were not considered in the studies presented here, but the results of the magnetic measurements are available and will be included in future analyses. Only the FQ of MQXFAs, MQXFBs, and MBRDs have been considered in the sorting analyses discussed later.

BEAM DYNAMICS IMPLICATIONS OF THE FIELD QUALITY OF Q1/Q3

The Q1 and Q3 quadrupoles, part of the inner-triplets of IR1 and IR5 [1], are each made by two MQXFA magnets, for a total of eight slots in the LHC ring that have to be filled with CAs from the pool of available units. The limited size of the magnet inventory and the large value of the β-functions at the corresponding ring locations make the choice of where to place each unit a non-trivial optimisation problem, which builds on previous HL-LHC IR-magnet sorting studies [17]. The methodology developed for sorting the MQXFBs [18], based on the use of the b_4 harmonic, is naturally extended to the case Q1/Q3 using the complete measured FQ of every magnet.

The eight Q1/Q3 slots of the HL-LHC are labelled by the side of the IP they sit on (L5, R5, L1, R1) and by their family type (Q1 or Q3). The set of admissible permutations is constructed taking into account the production status of the CAs at the time of this study (e.g. CA03 and CA08 are defined as being of family type Q1 while CA04, CA05 and CA09 are defined as being family type Q3).

The combination of these rules and constraints generates about 200 admissible permutations that define the available sorting space. For each permutation, the complete measured FQ content of every CA is installed in the HL-LHC Xsuite [22–24] lattice [25]. The MQXFA units used for this study are those for which the FQ is derived from the vertical measurements. The Q2 slots are considered to be filled with the recommended configuration according to the results of the studies performed independently [18], so that the Q1/Q3 permutations are studied with an already optimised layout of the Q2 quadrupoles.

Although the Q2 study focused on the analytical estimation of the amplitude detuning generated by the b_4 component alone, the analysis of the Q1/Q3 sorting retains the contribution of all the measured multipoles. The amplitude detuning coefficients $a_{xx}(J_x, J_y)$, $a_{yy}(J_x, J_y)$, $a_{xy}(J_x, J_y)$ and $a_{yx}(J_x, J_y)$ for each of the two beams are extracted directly from 4D tracking simulations performed with Xsuite [24]. Since the full FQ is retained, these coefficients are generally functions of transverse actions, and the corresponding detuning is therefore calculated at a specific point in action space.

The figure of merit is the two-beam norm [18]:

$$\|\mathbf{D}_{\text{B1,B2}}(J_x, J_y)\| = \sqrt{\|\mathbf{D}_{\text{B1}}(J_x, J_y)\|^2 + \|\mathbf{D}_{\text{B2}}(J_x, J_y)\|^2},$$

where $\|\mathbf{D}_{\text{Bi}}(J_x, J_y)\|^2 = a_{xx}^2(J_x, J_y) + a_{yy}^2(J_x, J_y) + a_{xy}^2(J_x, J_y) + a_{yx}^2(J_x, J_y)$. Following typical commissioning procedures based on AC-dipole excitations [26, 27], the detuning norm $\|\mathbf{D}_{\text{B1,B2}}(J_x, J_y)\|$ is evaluated at 2.5 σ. It is worth noting that the full FQ leads to a non-linear detuning with amplitude, so the ranking of the permutations depends on this choice. The evolution of $\|\mathbf{D}_{\text{B1,B2}}(J_x, J_y)\|$ as a function of the action is shown in Fig. 2.

At the chosen amplitude, the distribution of the two-beam detuning norm across admissible permutations spans roughly a factor of 3.7, from a best value of $\|\mathbf{D}_{\text{B1,B2}}\| = 2.33 \times$

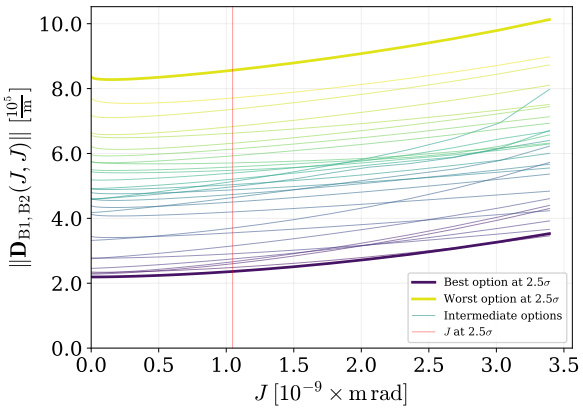

Figure 2: $\|\mathbf{D}_{\mathrm{B1,B2}}(J,J)\|$ as a function of J. Ranking depends on the amplitude used for the optimisation.

$10^5\ \mathrm{m}^{-1}$ to a worst value of $8.55 \times 10^5\ \mathrm{m}^{-1}$, with a median of $5.00 \times 10^5\ \mathrm{m}^{-1}$.

The recommended Q1/Q3 sorting, summarised in Table 2, minimises $\|\mathbf{D}_{\mathrm{B1,B2}}(J_x, J_y)\|$. The dominant detuning coefficients for this option, given as $(a_{xx}, a_{xy}, a_{yx}, a_{yy})$ in units of $10^5\ \mathrm{m}^{-1}$, are (0.4, 0.7, 0.7, −0.6) for B1 and (0.8, 0.9, 0.9, 2.0) for B2. The 13 best permutations all share the same Q3 sub-assignment for the R1 and R5 slots, namely CA09 at R1 and CA05 at R5: this is the dominant constraint of the Q1/Q3 sorting, and any layout that breaks it falls outside the top-13 and pays a steep penalty in $\|\mathbf{D}_{\mathrm{B1,B2}}(J_x, J_y)\|$. In contrast, the existence of a 13-permutation plateau gives the project operational flexibility: even if scheduling considerations or hardware issues were to forbid the global optimum, any of the 13 leading permutations remains within roughly 13% of the best value and well below the global median, providing a robust fall-back solution for the sorting.

Table 2: Recommended Q1/Q3 sorting. Each entry is the CA assigned to that type and side.

Type	L5	R1	R5	L1
Q1	CA07	CA03	CA08	CA06
Q3	CA10	CA09	CA05	CA04

IMPACT OF THE a_2 COMPONENT IN THE D2 MAGNETS ON HL-LHC OPTICS

The HL-LHC optics can be significantly affected (luminosity drop of the order of percent) by the field quality of the D2 recombination dipoles and their orbit correctors, in particular by the skew-quadrupole component (a_2) when the difference between the two apertures exceeds 2×10^{-4} (2 units) [28]. The figures of merit are the local coupling resonance driving term $|f_{1001}|$ at the interaction point (IP) and the CCs, and the global coupling coefficient $|C^-|$, with operational targets set to $|f_{1001}| < 0.01$ and $|C^-| < 0.001$. Correction relies on the two single-aperture skew quadrupole correctors close to the D1 separation dipole of each IR. These correctors provide a local compensation (an over-constrained problem with 2 free variables for 6 constraints) and on the arc skew quadrupoles for a global compensation. Hence, large aperture-to-aperture a_2 asymmetries are difficult to compensate, and this is the case for MBRD3 in the LMBRD04 CA, where the difference reaches almost 5 units.

Using the measured FQ at cold or the extrapolated FQ from warm measurements, all combinations of four CAs placed left and right of IR1 and IR5 were simulated. The four-digit sequences (e.g. 2513) used below indicate the four D2 CAs placed at L1, R1, L5 and R5, respectively. Figure 3 shows the mean $|f_{1001}|$ (yellow) and the mean absolute relative powering of the arc skew quadrupoles (red) for the configurations including LMBRD05. With LMBRD05 in the 2513 arrangement and at $+3\sigma$ errors, the configuration yields $|f_{1001}| \simeq 0.007$ and $|C^-| \simeq 1.86 \times 10^{-4}$ (B1), 1.83×10^{-4} (B2), well within the limits and without overpowering the arc skew quadrupoles. However, the same scan with the spare LMBRD04 CA is dominated by the large a_2 asymmetry of MBRD3 (findings presented in Ref. [29]): even the best ordering 4312 gives $|f_{1001}| \simeq 0.025$ and $|C^-| \simeq 4.68 \times 10^{-4}$ (B1), 4.24×10^{-4} (B2), all above the local threshold of 0.01, and no sorting recovers the cancellation between left and right of the IRs.

The recommended D2 configuration is given by the four-digit number 2513 and LMBRD04 is kept as a spare D2.

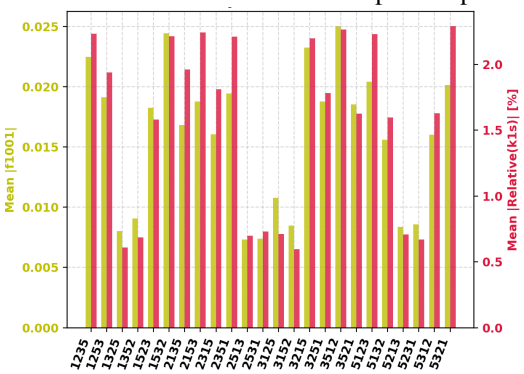

Figure 3: Mean $|f_{1001}|$ for both beams at the IP and the CC (yellow) and mean absolute relative powering of the arc skew quadrupoles (red), for the configurations with LMBRD05.

CONCLUSIONS

The production of the magnets for the HL-LHC is in full swing, as is the detailed programme of magnetic measurements to characterise the field quality of the new magnets for the high-luminosity insertions of the HL-LHC. The essential information has been used to optimise the assigments of the Q2 magnets and in this paper we have presented the sorting approach of the Q1/Q3 quadrupoles and that of the D2 recombination dipoles. The next step will be the study of the sorting options for the D1 separation dipoles, which will conclude the magnet allocation process for the HL-LHC.

ACKNOWLEDGEMENTS

The authors thank the WP2 and WP3 colleagues of the HL-LHC project for their valuable discussions.

REFERENCES

[1] O. Aberle *et al.*, *High-Luminosity Large Hadron Collider (HL-LHC): Technical design report*. Geneva: CERN, 2020. doi:10.23731/CYRM-2020-0010

[2] O. Brüning and L. Rossi, *The High Luminosity Large Hadron Collider*, O. Brüning, Ed. World Scientific, 2024. doi:10.1142/13487

[3] M. Li and S. Ohnuma, "Two-Parameter Sorting of Dipoles in Large Synchrotrons", in *Proc. EPAC'90*, Nice, France, Jun. 1990, pp. 1175–1178.

[4] V. Ziemann, "Sorting the LHC Dipoles using Simulated Annealing", in *Proc. EPAC'94*, London, UK, Jun.-Jul. 1994, pp. 1054–1057.

[5] M. Giovannozzi, R. Grassi, W. Scandale, and E. Todesco, "Sorting approach to magnetic random errors", *Phys. Rev. E*, vol. 52, no. 3, pp. 3093–3101, Sep. 1995. doi:10.1103/PhysRevE.52.3093

[6] D. Dinev, "Magnet Sorting Algorithms", in *Proc. EPAC'96*, Sitges, Spain, paper TUP045G, pp. 1374–1376, Sep. 1996.

[7] R. Bartolini, W. Scandale, M. Giovannozzi, and E. Todesco, "Sorting Strategies for the CERN-LHC Dipoles", in *Proc. PAC'97*, Vancouver, Canada, May 1997, paper 2V034, pp. 1469–1471.

[8] C. H. Chang, T. C. Fan, I. Hsu, C. S. Hwang, and C. Wang, "Magnet Sorting Algorithms for the SRRC EPU5.6", in *Proc. EPAC'98*, Stockholm, Sweden, paper MOP31G, pp. 2219–2221, Aug. 1998. https://jacow.org/e98/papers/MOP31G.pdf

[9] J. Wei *et al.*, "Real-World Sorting of RHIC Superconducting Magnets", in *Proc. PAC'99*, New York, NY, USA, Mar. 1999, paper THP95, pp. 3176–3178. https://jacow.org/p99/papers/THP95.pdf

[10] X. R. Resende and R. M. Dias, "Magnet Sorting Algorithm Applied to the LNLS EPU", in *Proc. EPAC'04*, Lucerne, Switzerland, paper MOPKF004, pp. 303–305, Sep. 2004. http://accelconf.web.cern.ch/e04/papers/MOPKF004.pdf

[11] D. Raparia, A. V. Fedotov, Y. Y. Lee, and J. Wei, "Dipole and Quadrupole Sorting for the SNS Ring", in *Proc. EPAC'04*, Lucerne, Switzerland, paper TUPLT189, pp. 1574–1576, Sep. 2004. http://accelconf.web.cern.ch/e04/papers/TUPLT189.pdf

[12] S. Peggs, E. Laface, E. Sargsyan, and R. Zeng, "Sorting in the ESS", in *Proc. IPAC'14*, Dresden, Germany, Jun. 2014, pp. 3329–3331. doi:10.18429/JACoW-IPAC2014-THPME047

[13] Y. Peng, J. Pan, and J. X. Zhou, "Study on magnets sorting for the HEPS booster", in *Proc. IPAC'23*, Venice, Italy, pp. 1088–1090, Sep. 2023. doi:10.18429/JACoW-IPAC2023-MOPM044

[14] S. D. Fartoukh, "Installation Strategy for the LHC Main Dipoles", in *Proc. EPAC'04*, Lucerne, Switzerland, paper WEOALH03, pp. 176–178, Sep. 2004. http://accelconf.web.cern.ch/e04/papers/WEOALH03.pdf

[15] P. Bestmann *et al.*, "Magnet Acceptance and Allocation at the LHC Magnet Evaluation Board", in *Proc. PAC'07*, Albuquerque, NM, USA, paper FROAKI01, pp. 3739–3741, Aug. 2007. https://jacow.org/p07/papers/FROAKI01.pdf

[16] S. Fartoukh and M. Giovannozzi, "Dynamic aperture computation for the as-built CERN Large Hadron Collider and impact of main dipoles sorting", *Nucl. Instrum. Methods Phys. Res., A*, vol. 671, pp. 10–23, 2011. doi:10.1016/j.nima.2011.12.052

[17] T. Pugnat, A. Wegscheider, E. Todesco, M. Giovannozzi, and R. Tomas, "Sorting strategies for the new superconducting magnets for the CERN HL-LHC", in *Proc. IPAC'24*, Nashville, TN, USA, pp. 3003–3006, Jul. 2024. doi:10.18429/JACoW-IPAC2024-THPC16

[18] A. Fornara, M. Giovannozzi, and G. Sterbini, "Current classification strategies based on the transfer function and field quality of the new superconducting magnets in the HL-LHC", presented at the 17th International Particle Accelerator Conference (IPAC'26), Deauville, France, May 2026, this conference.

[19] G. Ambrosio *et al.*, "Q1/Q3 Integrated Field and Field Quality", https://indico.cern.ch/event/1559978/contributions/6664969/attachments/3146848/5587625/Q1Q3-IntegratedGradientAndFieldQuality.pdf

[20] J. Doyle *et al.*, "Evaluation of the Room Temperature Field Quality Measurements of HL-LHC MQXFA Magnet Assemblies", *IEEE Trans. Appl. Supercond.*, vol. 36, no. 3, pp. 1–6, 2026. doi:10.1109/TASC.2026.3658305

[21] S. I. Bermudez *et al.*, "Status and Challenges in the MQXFB Nb3Sn Quadrupoles for the HL-LHC", *IEEE Trans. Appl. Supercond.*, vol. 35, no. 5, pp. 1–7, 2025. doi:10.1109/TASC.2025.3530911

[22] G. Iadarola *et al.*, Xsuite, https://xsuite.readthedocs.io

[23] G. Iadarola *et al.*, "Xsuite: an integrated beam physics simulation framework", in *Proc. 68th Adv. Beam Dyn. Workshop High-Intensity High-Brightness Hadron Beams (HB'23), Geneva, Switzerland*, pp. 73–80, 2023. doi:10.18429/JACoW-HB2023-TUA2I1

[24] G. Iadarola *et al.*, "Xsuite: an integrated beam physics simulation framework", in *Proc. IPAC'24*, Nashville, TN, pp. 2623–2626, May 2024. doi:10.18429/JACoW-IPAC2024-WEPR56

[25] "HL-LHC Lattice Version 19", GitLab repository at https://gitlab.cern.ch/acc-models/acc-models-lhc/-/tree/hl19, 2026,

[26] E. H. Maclean *et al.*, "New approach to LHC optics commissioning for the nonlinear era", *Phys. Rev. Accel. Beams*, vol. 22, no. 6, p. 061004, Jun. 2019. doi:10.1103/PhysRevAccelBeams.22.061004

[27] F. S. Carlier, R. Tomás, E. H. Maclean, and T. H. B. Persson, "First experimental demonstration of forced dynamic aperture measurements with LHC ac dipoles", *Phys. Rev. Accel. Beams*, vol. 22, no. 3, p. 031002, Mar. 2019. doi:10.1103/PhysRevAccelBeams.22.031002

[28] R. Tomas, "Optimizing the global coupling knobs for the LHC", 2012. https://cds.cern.ch/record/1422434

[29] K. Skoufaris, A. Fornara, E. H. Maclean, G. Iadarola, R. D. Maria, and R. T. García, "D2 magnets: proposed configuration", https://indico.cern.ch/event/1668160/contributions/7013104/attachments/3248468/5797139/D2%20magnets_%20proposed%20configuration.pdf